

Bonding Modes in the Analogous and Isoelectronic Group VB/VA Compounds $\text{As}(\text{O})\text{Cl}_3$ and $\text{Nb}(\text{O})\text{Cl}_3$

An Ultraviolet Photoelectron-spectroscopic and SCC- $X\alpha$ Study

BY SUSANNE ELBEL,* ANDREAS BLANCK AND HORST WALTHER

Institut für Anorganische und Angewandte Chemie, Universität Hamburg,
D-2000 Hamburg 13, Federal Republic of Germany

AND MICHAEL GRODZICKI

Institut für Theoretische Physik, Universität Hamburg, D-2000 Hamburg 13,
Federal Republic of Germany

Received 30th July, 1984

The He I α photoelectron spectra of gaseous 'non-existent' $\text{As}(\text{O})\text{Cl}_3$ and of $\text{Nb}(\text{O})\text{Cl}_3$ have been compared and assigned using the SCC- $X\alpha$ method. In order to confirm the interpretation, correlations with the known ionization potentials of isomorphous $\text{P}(\text{O})\text{Cl}_3$ and $\text{V}(\text{O})\text{Cl}_3$, respectively, are considered. Differences in bonding modes are discussed and illustrated with respect to the SCC- $X\alpha$ population analyses, to the relative central atomic orbital contributions, to the atomic energy levels and to the experimental ionization energies of the parent AsCl_3 and PCl_3 .

Apart from their unique capability of coordinating carbon monoxide and related neutral ligands, transition metals also form a great variety of compounds possessing isomorphous counterparts in the corresponding main-group sections, e.g. $\text{TiCl}_4/\text{SnCl}_4$, $\text{TaMe}_5/\text{SbMe}_5$, $\text{V}_4\text{O}_{10}/\text{P}_4\text{O}_{10}$ etc. A discussion of the bonding differences between such analogues is still missing from the literature, although a range of comparative photoelectron-spectroscopic investigations have been published.¹⁻³ These contributions have mainly dealt with band assignments. It is the purpose of our present study to give information about the bonding properties of a representative pair of analogous group B and group A compounds by means of qualitative molecular-orbital considerations mediated by a new photoelectron-spectroscopy-adjusted semi-empirical technique, SCC- $X\alpha$.⁴ This method has already proved useful in the description of bonding properties for a large selection of compounds containing light or heavy elements⁵ and particularly for the complete set of the known Group V trihalides.^{5b} We have chosen two simple Group V compounds unknown to photoelectron spectroscopists so far: the 'non-existent' short-lived compound $\text{As}(\text{O})\text{Cl}_3$, first detected by Seppelt *et al.* in 1978,⁶ and the high-temperature $\text{Nb}(\text{O})\text{Cl}_3$ monomer. This particular pair has several advantages when considering the possibility of examining (i) two different modes of bonding within the same molecule, *i.e.* the covalent polar E—Cl and the semi-polar, or even retrodative, E—O bonds and (ii) the extent of *d*-orbital participation in bonding for both VB/VA counterparts and the use of 'heavy-atom effects' within both groups. Additionally, $\text{V}(\text{O})\text{Cl}_3$ ⁷ and $\text{P}(\text{O})\text{Cl}_3$ ⁸ are well known to both photoelectron spectroscopists and theoreticians and could serve as valuable reference systems by helping to clarify problems which might arise from the photoelectron spectra of their heavier congeners.

EXPERIMENTAL

Arsenic oxytrichloride was prepared according to the method of Seppelt *et al.*⁶ by ozonizing AsCl_3 , dissolved in CH_2Cl_2 , at -78°C . Solid $\text{As}(\text{O})\text{Cl}_3$ was separated from the liquid phase by simply decanting the solvent. The colourless, wet precipitate was kept in dry ice throughout the whole procedure [$\text{As}(\text{O})\text{Cl}_3$ is known to decompose and to form involatile $(\text{As}_2\text{O}_3\text{Cl}_4)_x$ at temperatures $> -30^\circ\text{C}$].⁶ The reaction flask was then connected with the inlet of the photoelectron spectrometer. For 5–7 h while the sample reservoir was allowed to warm up to room temperature, test spectra were recorded. Besides the more or less superimposed spectra of CH_2Cl_2 , Cl_2 and AsCl_3 in the early stage of the measurement, several pure photoelectron spectra of a new species, later identified as $\text{As}(\text{O})\text{Cl}_3$, could be recorded within a period of 10–15 min just before the reaction mixture reached room temperature and before the sample had obviously decomposed. The whole procedure, including the preparation of new starting material using alternant solvents,⁶ was repeated twice.

$\text{Nb}(\text{O})\text{Cl}_3$ was prepared from NbCl_5 by infrared-spectroscopic-controlled exposure to air. It was sublimed into the ionization chamber of the spectrometer using an electrically heated sample rod equipped with a stainless-steel crucible at the top. A maximum furnace temperature of $>400^\circ\text{C}$ at 10^{-4} mbar was required. Gaseous $\text{Nb}(\text{O})\text{Cl}_3$ was introduced into the collision chamber through a hot inlet pipe (Mo, diameter 5 mm, *ca.* 850°C).

The He I photoelectron spectra were recorded using a UPG 200 spectrometer from Leybold-Heraeus GmbH Cologne and were calibrated with argon. The resolution ranged from 25 to 30 meV in both cases with an estimated accuracy of ± 0.10 eV for the ionization energies.

COMPUTATIONAL REQUIREMENTS

Grodzicki's SCC- $X\alpha$ method, described fully elsewhere,^{4,5} was applied using trial geometries for $\text{E}(\text{O})\text{Cl}_3$. Bond distances and valence angles were estimated from the known geometries of VOCl_3 ,⁹ AsCl_3 ,¹⁰ $\text{PCl}_3/\text{POCl}_3$ ¹¹ and $(\text{NbOCl}_3\cdot\text{POCl}_3)_4$.¹² Optimized SCC- $X\alpha$ parameters for the atoms of concern were obtained by fitting calculated orbital energies for the elements E_2/E_4 ($E = \text{P}$ or As), Cl_2 and the diatomic interhalogens to experimental ionization energies or by using known atomic values for Nb, V and O. The SCC- $X\alpha$ program was amplified by the PSI/77¹³ and FPLOT^{1b} subroutines to plot valence-electron densities or wavefunctions. The SCC- $X\alpha$ calculations were accompanied by CNDO/II (main-group compounds) and extended Hückel calculations. For the extended Hückel basis double-zeta STO exponents and H_{ii} energies for V and Nb were taken from the literature.¹⁴ Standard values were used for P, As, Cl and O.¹⁵ The relative extended Hückel α parameters for the atoms involved are shown in fig. 1.

RESULTS AND DISCUSSION

The assigned He I photoelectron spectra of the $\text{E}(\text{O})\text{Cl}_3$ series ($E = \text{P}$, As , Nb , or V) are shown in fig. 2. The spectrum of VOCl_3 was taken from the literature.⁷ Vertical ionization energies are summarized in table 1.

Although the four oxides are isosteric there is an apparent dissimilarity between the band envelopes and patterns of fig. 2. Photoelectron bands of $\text{P}(\text{O})\text{Cl}_3$ and $\text{As}(\text{O})\text{Cl}_3$ are distributed over a broader energy range (*ca.* 11–17 eV), whereas the bands of the transition-metal analogues span nearly 3 eV. Additionally, the latter show smaller half-widths. The different energy distributions for the valence molecular orbitals of the main-group in contrast to the transition-metal compounds may be traced back to the energy patterns of the central atoms depicted in fig. 1; however, for a more thorough inspection of the molecular-orbital characteristics associated with the photoelectron energies more information is needed.

All four oxides belong to the C_{3v} molecular point group and possess sixteen occupied valence molecular orbitals which transform as $5 \times a_1$, $1 \times a_2$ and $5 \times e$. The

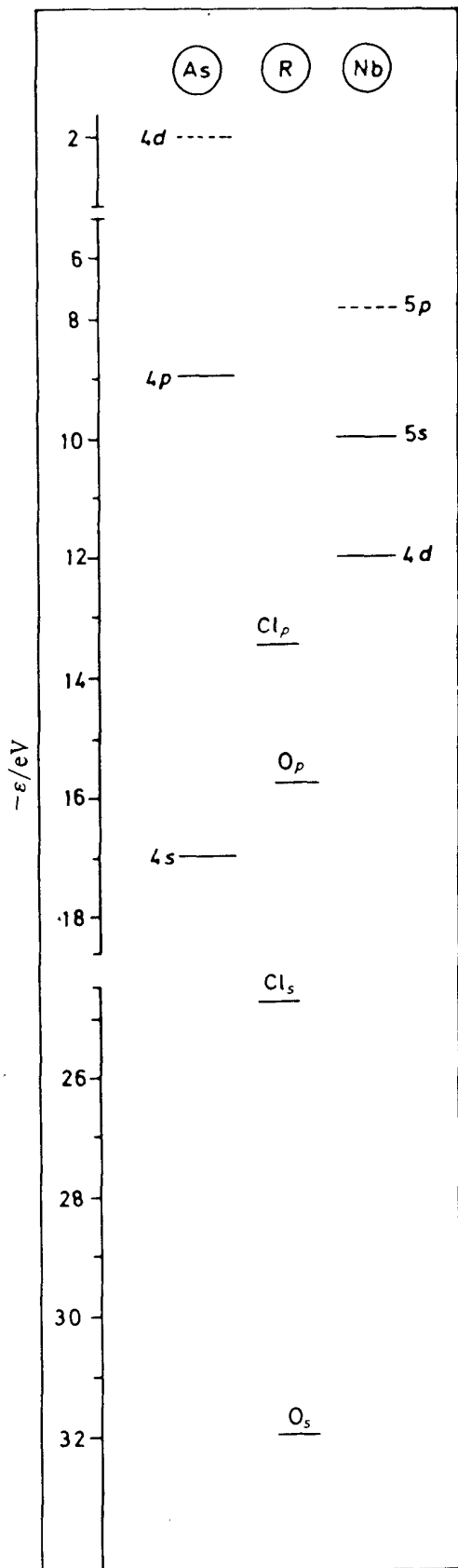


Fig. 1. Relative positions of valence shell ionization potentials ($H_{ii}^{14,15}$) of Nb, As, O and Cl.

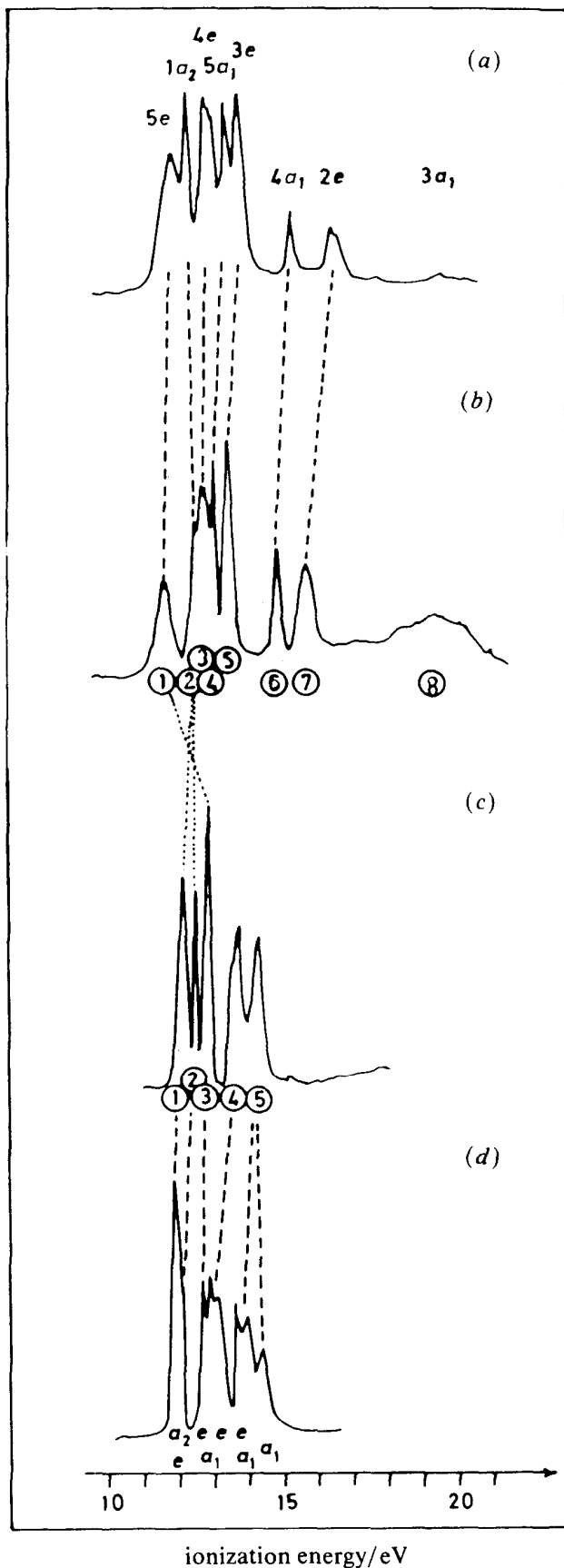


Fig. 2. He I α photoelectron spectra of the isosteric series (a) P(O)Cl₃, (b) As(O)Cl₃, (c) Nb(O)Cl₃ and (d) V(O)Cl₃ with assignment.

Table 1. Experimental ionization potentials (band maxima), SCC-X α eigenvalues and orbital compositions for PCl₃, AsCl₃, P(O)Cl₃, As(O)Cl₃, V(O)Cl₃ and Nb(O)Cl₃

	P/V					As/Nb				
	exptl	SCC-X α	% E	% Cl	% O	exptl	SCC-X α	% E	% Cl	% O
ECl ₃ ^a										
4a ₁	10.5	11.36	56	44		10.85	11.17	48	52	
1a ₂	11.7	12.04	—	100		} 11.66	11.62	—	100	
4e	12.0	12.24	1	99			11.79	1	99	
3e	12.92	13.25	1	99			12.54	12.77	1	99
3a ₁	14.24	14.18	24	76		13.63	13.83	27	73	
2e	15.22	15.51	21	79		14.56	15.11	20	80	
2a ₁	18.85	19.57	32	68			20.18	35	65	
P(O)Cl ₃ /As(O)Cl ₃ ^b										
5e	11.89	11.68	5	23	72	11.65	11.39	8	24	68
1a ₂	12.38	12.54	—	100	—	12.50	12.08	—	100	—
4e	12.98/13.09	13.03	2	91	7	12.77	12.55	3	87	10
5a ₁	13.47	13.96	4	78	18	13.08	13.53	4	82	14
3e	13.85	14.02	1	98	1	13.47	13.46	2	97	1
4a ₁	15.35	15.10	4	23	73	14.85	14.85	5	21	74
2e	16.53	16.63	24	73	3	15.73	15.90	21	77	2
3a ₁	19.55	19.74	19	72	9	~19.5	19.99	21	66	13
V(O)Cl ₃ /Nb(O)Cl ₃										
5e	} 11.84	11.74	3	81	16	12.14	12.28	1	74	25
1a ₂		11.72	—	100	—	12.50	12.38	—	100	—
5a ₁	12.65	12.88	11	89	—	} 12.89	13.14	6	93	1
4e	12.91/13.08	12.84	15	84	1		13.19	8	86	6
3e	13.65	13.40	27	25	48	} 13.76	13.53	17	33	50
4a ₁	13.90	14.69	21	37	42		14.14	12	8	80
2e	14.35	14.26	13	74	13	14.32	14.48	18	82	—
3a ₁		15.60	1	54	45		14.85	2	85	13

^a Without *d* orbitals in the basis set; ^b including *d* orbitals in the basis set.

central *s*, *p* and *d* valence atomic orbitals of E in E(O)X₃ (where X is a halogen), which are more or less involved in σ - or π -type bonding, transform as *s*, *p_z*, *d_z²*: *a₁*; *p_x*/*p_y*; *d_x²-*y*²*/*d_{xy}*; *d_{xz}*/*d_{yz}*: *e* under molecular symmetry. The unique 1a₂ molecular orbital which remains when assembling the matching atomic orbitals of E, O and Cl₃ to yield molecular orbitals shows pure halogen *p* character (Cl_p) for symmetry reasons. The photoelectron spectra of V(O)Cl₃⁷ and P(O)Cl₃⁸ have frequently been discussed in the literature. In contrast to V(O)Cl₃ or V(O)F₃,^{7b} where criteria gained from relative band intensities do not help in clarifying the underlying energy patterns, the P(O)Cl₃ photoelectron data have been assigned by comparison with the known PCl₃ photoelectron spectrum.⁸ There is no reason why the same should not hold for the AsCl₃/As(O)Cl₃ pair [for AsCl₃ see ref. (5b) and references therein]. The photoelectron band pattern of As(O)Cl₃ will therefore be interpreted with respect to the He I α photoelectron spectrum of AsCl₃^{5b} and by comparison with the POCl₃ spectrum⁸ (see fig. 2) with the aim that the two versions should complement one another. The photoelectron spectrum of Nb(O)Cl₃ is

interpreted with regard to the photoelectron data of its lighter counterpart $V(O)Cl_3$ ⁷ applying the heavy-atom effect, which has been well defined in photoelectron spectroscopy of homologous transition-metal compounds.¹⁶ Since it is our intention to deduce the main bonding differences between corresponding transition-metal and main-group species, exemplified here with the pair $As(O)Cl_3/Nb(O)Cl_3$, on the basis of the assigned photoelectron data and by means of SCC- $X\alpha$ calculations, we shall also give an overall view on valence-electron densities and overlap charges. This is because the SCC- $X\alpha$ method has proved to be competitive, or even more 'realistic' in terms of photoelectron energies, than more expensive $X\alpha$ methods and semi-empirical methods.^{1,4,5}

The photoelectron energy sequences of $P(O)Cl_3$ and hence $As(O)Cl_3$ can be rationalized by admitting a strong charge migration from E to O on forming the semi-polar $E \rightarrow O$ bond and by evaluating the effect of this on each original ECl_3 energy level. (The geometry change of the ECl_3 skeleton accompanying this process is of minor importance.) The overall effect, which may be described in terms of stabilizing or destabilizing hyperconjugative and/or inductive contributions onto the $AsCl_3$ molecular orbitals, is shown in fig. 3(a). The formation of $As(O)Cl_3$ from $AsCl_3$ is simulated by SCC- $X\alpha$ energies and by wavefunction plots. The effect of including As d atomic orbitals in $As(O)Cl_3$ is also incorporated: The 5e HOMO is affected most, now gaining π_{As-O} -bonding character, synonymous with the formation of a retrodative semi-polar $E=O$ bond. [The corresponding $As(O)Cl_3$ wavefunction plots which will be discussed below are given in fig. 3(c).] The main characteristics are as follows. (i) On going from $As^{(III)}$ to $As^{(V)}$ there is an overall high-energy σ_{As-Cl} band group (bands 6 and 7 or $2e$ and $4a_1$) on introducing lone-pair energy n_{As} of $AsCl_3$ now involved in σ_{As-O} -bond formation [$4a_1 \rightarrow 5a_1$ and $4a_1$, bands 4 and 6 in fig. 2, cf. fig. 3(a)]. (ii) Comparing the photoelectron data of $AsCl_3$ and $As(O)Cl_3$ (table 1), the degenerate n_O HOMO (band 1 in fig. 2) supercedes n_{As} , the HOMO of $AsCl_3$, centred at 10.85 eV. (iii) Typical n_{Cl} bands ($4e$, $1a_2$ and $3e$, or bands 2, 3 and 5, respectively, in fig. 2) are shifted less than the high-energy σ_{As-Cl} band group (bands 6 and 7 or $2e$ and $4a_1$) on introducing oxygen, favouring the view of appreciable electrostatic contributions to the new $E=O$ bond. (iv) The $\Delta 1a_2$ energy shift might serve as an internal measure of the size of the charge transfer (inductive effect). As expected and owing to the greater bond polarities in arsenic compounds, governed by the larger atomic electronegativity differences, the $\Delta 1a_2$ shift is more pronounced for $AsCl_3 \rightarrow As(O)Cl_3$ (0.84 eV) than for $PCl_3 \rightarrow P(O)Cl_3$ (0.68 eV). The $1a_2$ band of $As(O)Cl_3$ (band 2 in fig. 2) is localized at 12.50 eV. Since the formation of the P—O coordinate bond by phosphane donors has been investigated by photoelectron spectroscopists and theoreticians several times,^{8,17} this change is illustrated here for the first time, and we will not dwell on it any longer. Note also that the $3a_1$ band has not been resolved for $As(O)Cl_3$, although some high-energy features (band 8 in fig. 2) are present.

Comparing both oxides $P(O)Cl_3$ and $As(O)Cl_3$ (upper part of fig. 2) it is obvious that the relevant energy area has shrunk for the latter, as is typical for the parent donors.^{5b} Among others this may be regarded as a consequence of decreasing atomic-orbital interactions between the atoms concerned with increasing atomic sizes. The n_O lone-pair band (band 1 in fig. 2) of $As(O)Cl_3$ is more destabilized in comparison with that of $P(O)Cl_3$, which is in accord with the higher polarity of the $As-O$ bond (table 2) and is not surprising. However, this is not the reason for the transient behaviour of $As(O)Cl_3$. Furthermore, the former n_E level of ECl_3 is much more stabilized for $E = P$ [$\Delta(4-5)a_1 = 2.97$ eV] than for the As compound [$\Delta(4-5)a_1 = 2.23$ eV], implying again a weaker σ bond here. Finally, the energy gap between

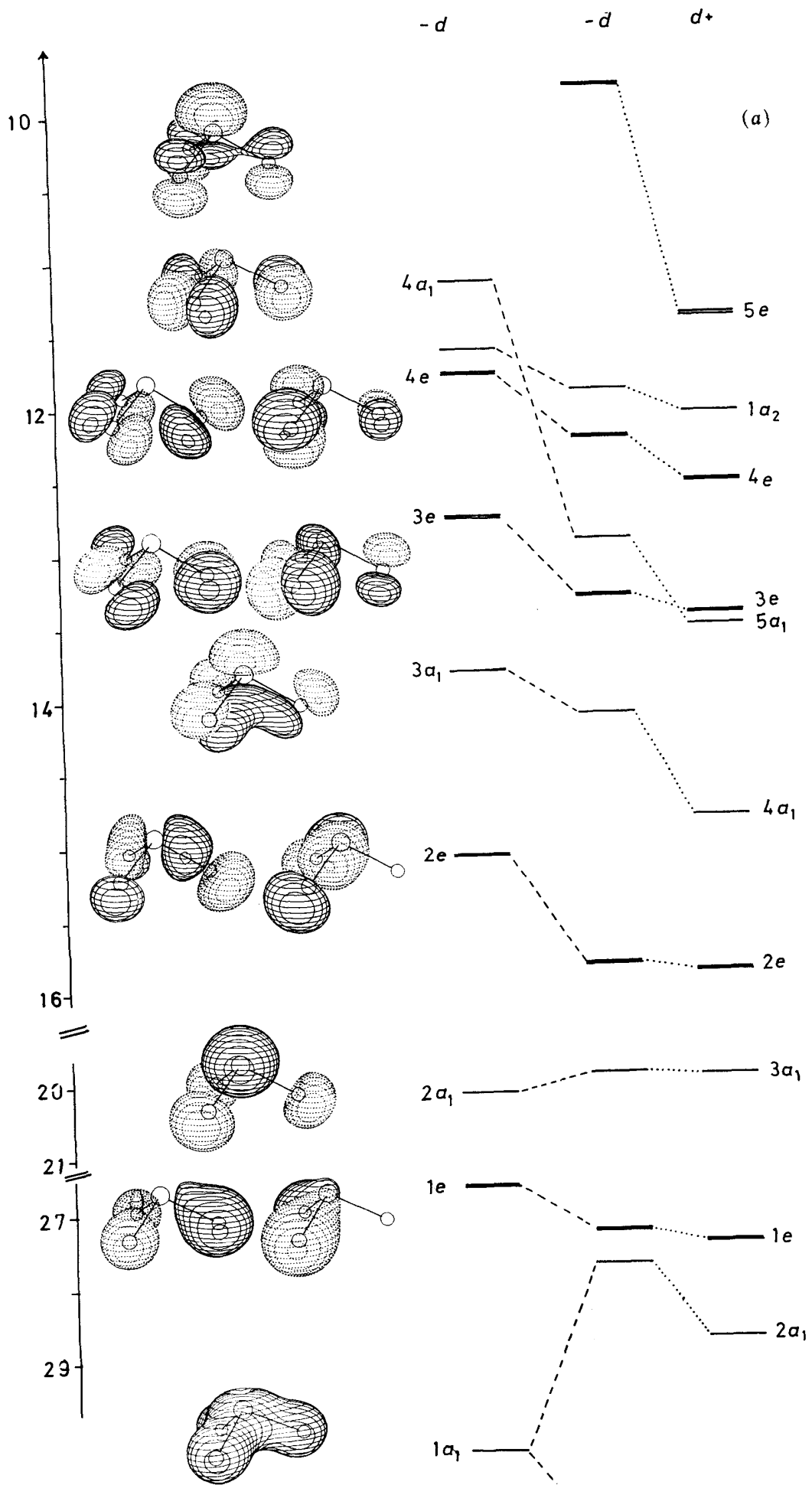


Fig. 3. For caption see over.

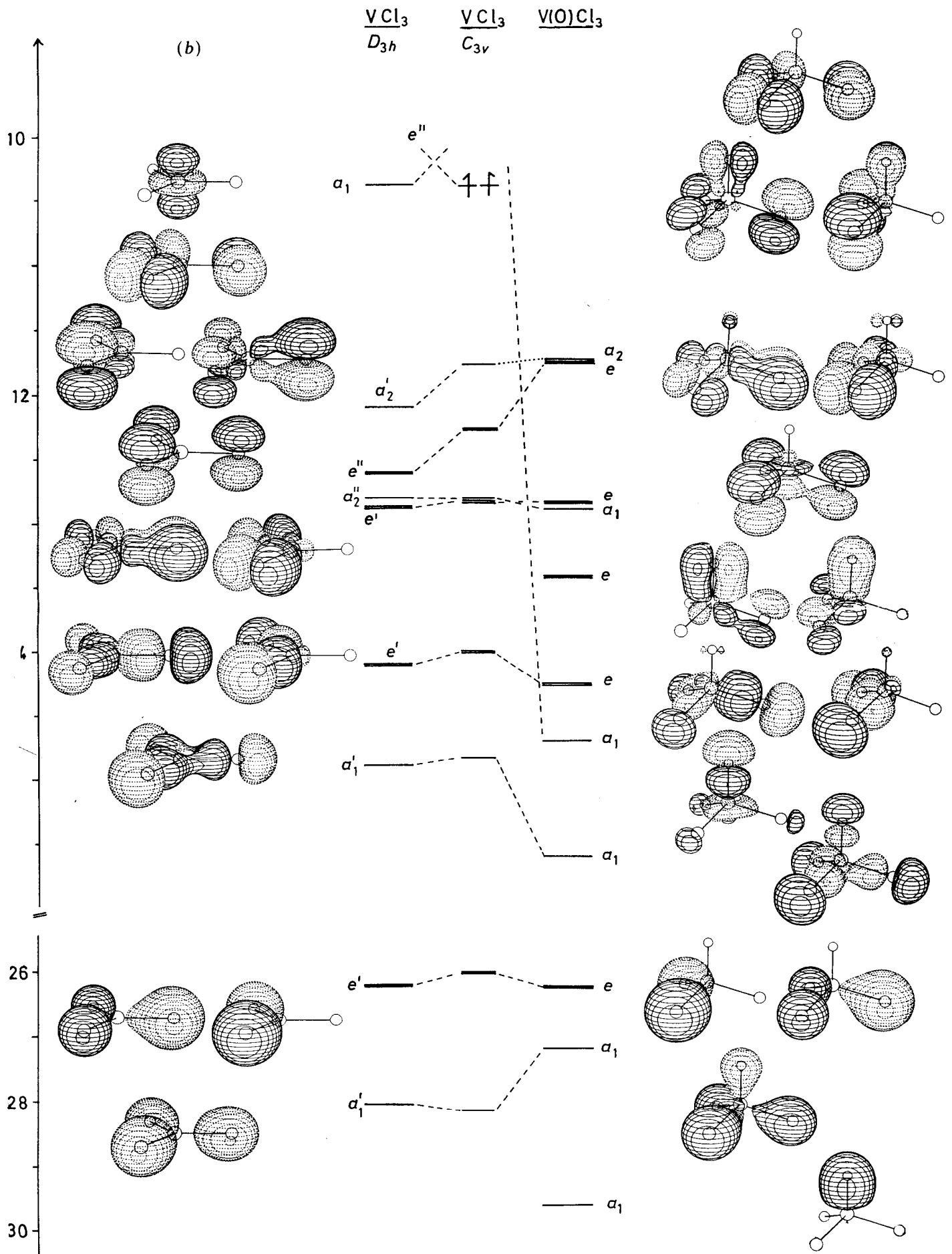


Fig. 3. (cont.)

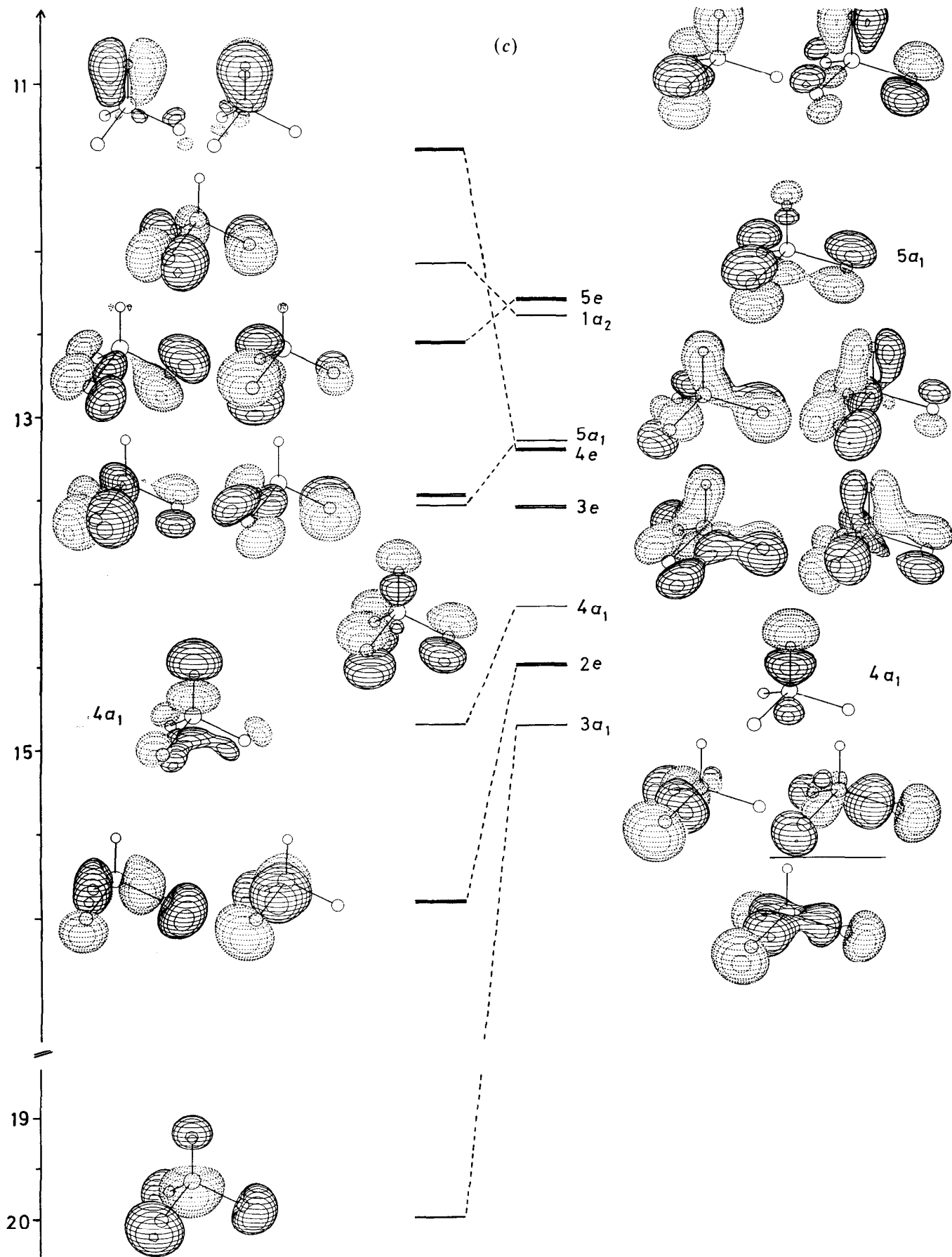


Fig. 3. (a) Correlation diagram for AsCl_3 and As(O)Cl_3 [calculated with (+ d) or without (- d) As d orbitals] with wavefunction plots for the arsane on the basis of SCC- $X\alpha$ calculations. (b) Orbital energy diagram for hypothetical VCl_3 (planar and pyramidal) and V(O)Cl_3 with wavefunction plots based on SCC- $X\alpha$ calculations. (c) Correlation diagram for isomorphous As(O)Cl_3 and Nb(O)Cl_3 based on SCC- $X\alpha$ eigenvalues and eigenfunctions for occupied valence molecular orbitals.

the two highest n_{Cl} levels of $\text{As}(\text{O})\text{Cl}_3$ ($1a_2$ and $4e$) decreases with increasing Cl—Cl distances hiding the a_2 band, which is still well separated for $\text{P}(\text{O})\text{Cl}_3$ (fig. 2), under band 3. Apart from these details, both spectra as well as the respective molecular-orbital compositions (table 1) show the same gross features. The molecular-orbital energy and ionization-energy sequences are retained for $\text{As}(\text{O})\text{Cl}_3$.

In contrast to the four main-group compounds mentioned above, where d orbitals on the central atoms play a minor rôle in bonding (all the photoelectron spectra can be completely assigned without taking any d atomic orbitals into account), the bonding in $\text{V}(\text{O})\text{Cl}_3$ and $\text{Nb}(\text{O})\text{Cl}_3$ is clearly determined by the d orbitals of vanadium and niobium. The situation is therefore much more complex and has presumably caused the problems associated with the photoelectron-spectroscopic analysis of $\text{V}(\text{O})\text{Cl}_3$,⁷ a commercial compound which is easy to record. spd hybrid orbitals have to be considered for symmetry and energy reasons (*cf.* fig. 1). The differing relative atomic-orbital energy patterns in fig. 1 seem to persist for the molecular-orbital energy or the respective photoelectron band distributions in fig. 2 and may be responsible for the apparent discrepancy between the photoelectron spectra of these formally isomorphous species from opposite sides of the periodic table. To describe the compositions of the occupied molecular orbitals of $\text{Nb}(\text{O})\text{Cl}_3$ and $\text{V}(\text{O})\text{Cl}_3$ we again prefer the pictorial presentations as shown in fig. 3(b) and (c). Fig. 3(b) is supposed to demonstrate how $\text{E}(\text{O})\text{Cl}_3$ molecular orbitals, exemplified with $\text{E} = \text{V}$, develop from hypothetical monomeric VCl_3 units in analogy to the transition $\text{AsCl}_3 \rightarrow \text{As}(\text{O})\text{Cl}_3$ in fig. 3(a). The problem associated with VCl_3 is the triplet ground state calculated for the C_{3v} geometry, and so the singlet planar case was preferred for correlation. (Note that there is no consensus in the literature concerning the geometries of monomeric transition-metal trifluorides.¹⁸) The molecular-orbital diagrams of $\text{V}(\text{O})\text{Cl}_3$ in fig. 3(b) demonstrate this marked influence of the central d orbitals in O—V—Cl bonding indicated above. The $\sigma_{\text{V-O}}$ bond is thus formed from the pure $\text{V}_{d_{z^2}}$ atomic orbital (HOMO of planar VCl_3), whereas the low-energy $5e$ orbital shows appreciable n_{Cl} character. The n_{Cl} predominance is present for the occupied frontier molecular orbitals (*cf.* table 1) and it is not surprising to find the $1a_2$ bands at the low-energy edge of both $\text{V}(\text{O})\text{Cl}_3$ ⁷ and $\text{Nb}(\text{O})\text{Cl}_3$ spectra (band 2 for the latter, fig. 2). Among the molecular-orbital types discussed in conjunction with He I photoelectron spectra, only $2e$ and $4a_1$ possess slight s and p character. The high-energy ionization energies, $3e$, $4a_1$ and $2e$, of $\text{Nb}(\text{O})\text{Cl}_3$ (bands 4 and 5 in fig. 2) are ascribed to molecular orbitals with strong bonding character and hence appreciable d atomic-orbital contributions, as suggested by the respective molecular-orbital compositions in table 1. Substituting vanadium by niobium should lead to better separation of those bands which are assigned to molecular orbitals possessing high d atomic-orbital contributions (the heavy-atom effect¹⁶). This is partly true for the low-energy region of $\text{Nb}(\text{O})\text{Cl}_3$ where $1a_2$ and $5e$ bands appear separated, but is more pronounced for the $4e/3e$ ($\pi_{\text{Nb-O}}$) photoelectron energy region, as expected from the results in table 1. In contrast to $\text{As}(\text{O})\text{Cl}_3$ and $\text{P}(\text{O})\text{Cl}_3$,⁸ where ionization energies referring to ionizations from molecular orbitals with high central s character (E_s) appear already in the He I region, none of the high-energy ionization energies referring to the $2a_1$, $1e$ or $1a_1$ valence molecular orbitals, as depicted for $\text{V}(\text{O})\text{Cl}_3$ in fig. 3(b), are expected to occur beneath 21 eV for the transition-metal oxychlorides. It is evident that their totally symmetric $1a_1$ molecular orbitals are composed almost entirely of the O_s atomic orbitals, in agreement with the energy scale in fig. 1. The respective molecular orbitals of $\text{P}(\text{O})\text{Cl}_3$ and $\text{As}(\text{O})\text{Cl}_3$ correlate mainly with E_s atomic orbitals. Since the $\text{V}(\text{O})\text{Cl}_3$ band pattern, a system of three separated band groups (fig. 2), is

reflected by the SCC- $X\alpha$ eigenvalues in fig. 3(b), which are in good agreement with the 2ph-computations of Pellach *et al.*,^{7b} we believe that the molecular-orbital presentation derived here is reasonable. There is a slight discrepancy between our SCC- $X\alpha$ energy sequence and the recently revised photoelectron-spectroscopic assignment for V(O)Cl₃^{7b} concerning the position of the σ_{V-O} -bonding molecular orbital $4a_1$; this ionization energy is calculated by 2ph-TDA,^{7b} LCAO- $X\alpha$ ^{7b} and our method to occur in the high-energy region, *i.e.* in the third band group at 14 eV. Since the He II assignment^{7b} is not convincing for this band we have little doubt about its location within the high-energy band complexes [band 5 for Nb(O)Cl₃, fig. 2]. From fig. 3(b) and (c) it is obvious that the V(O)Cl₃ and Nb(O)Cl₃ molecular orbitals are generally strongly mixed. In contrast to P(O)Cl₃ and As(O)Cl₃, the distinction between typical n_{Cl} and n_O levels is no longer present. The only correspondence is found for the $1a_2$ molecular orbital (n_{Cl}), implying that both bands in As(O)Cl₃ and Nb(O)Cl₃ should appear in the same energy region, since the atomic electronegativities of the central atoms do not vary very much.¹⁹ The respective bands have been correlated in fig. 2. Referring to our computational results (table 1 and fig. 3) the photoelectron spectrum of Nb(O)Cl₃ is assigned according to fig. 2 as follows. Band 1 corresponds with the $5e$ (n_{Cl}) molecular orbitals whereas the $1a_2$ level is ascribed to band 2 for intensity reasons.^{7b} Band 3 is also of high intensity and is assigned to ionizations from the $4e$ ($\pi_{O-Nb-Cl}$ bonding) and $5a_1$ molecular orbitals [slightly ($p-d$) π_{Nb-Cl} bonding]. Band 4 comprises $3e$ and possibly $4a_1$ ionization energies belonging to π_{O-Nb} and σ_{Nb-O} bonding molecular orbitals, respectively, whereas the $2e$ and $3a_1$ levels hidden underneath band 5 are ascribed to σ_{Nb-Cl} -bonding molecular orbitals. This might indicate another formal relationship with As(O)Cl₃, where σ_{As-Cl} levels are undoubtedly localized at higher ionization energies ($2e$ and $3a_1$ in fig. 2). The interpretation given here for Nb(O)Cl₃ and V(O)Cl₃ is substantiated by the photoelectron data for V(O)Br₃,^{1a} where band shifts with respect to V(O)Cl₃ and P(O)Cl₃/P(O)Br₃ have been evaluated to clarify the situation with V(O)Cl₃.

The contributions to the occupied valence molecular orbitals for E(O)Cl₃ molecules as shown in fig. 3(b) and (c) and as listed in table 1 indicate that the valence-bonding properties of V(O)Cl₃ or Nb(O)Cl₃ may be best described by overlap between metal d atomic orbitals and appropriate s - and p -type Cl₃-group orbitals. E_s and E_p valence orbitals do not contribute much in the low-energy region of the occupied molecular orbitals as a consequence of being repelled by the interaction with oxygen atomic orbitals. This phenomenon is also observed in band-structure calculations when comparing metallic vanadium²⁰ and VO²¹ (or NbO^{14b}). While in vanadium the $4s$ band is found *ca.* 6 eV below the d band at the centre of the Brillouin zone, the s band in VO is repelled because of the influence of oxygen. Therefore the s band lies above the Fermi level and is unoccupied. The situation is totally different for As(O)Cl₃ and the phosphorus analogue. Bond formation occurs with central valence p and s atomic orbitals, the diffuse d orbitals (*cf.* V and P $3d$ Slater exponents^{14,15}) being almost negligible. To illustrate this difference, valence-electron-density contour plots for V(O)Cl₃ and P(O)Cl₃ are shown in fig. 4. Besides the superficial similarity, the electron density is much more delocalized in P(O)Cl₃ particularly if the minus d version (designated $-d$) is considered. For this oxide the difference valence-electron-density contour is also plotted to show the influence of d orbitals on bonding: the P_d electron density is accumulated within the P—O bond region and less is found in the E—Cl bonding area. In V(O)Cl₃ the electron density is localized near the V nucleus if the V—Cl bond region only is examined. In table 2 effective atomic and overlap charges as

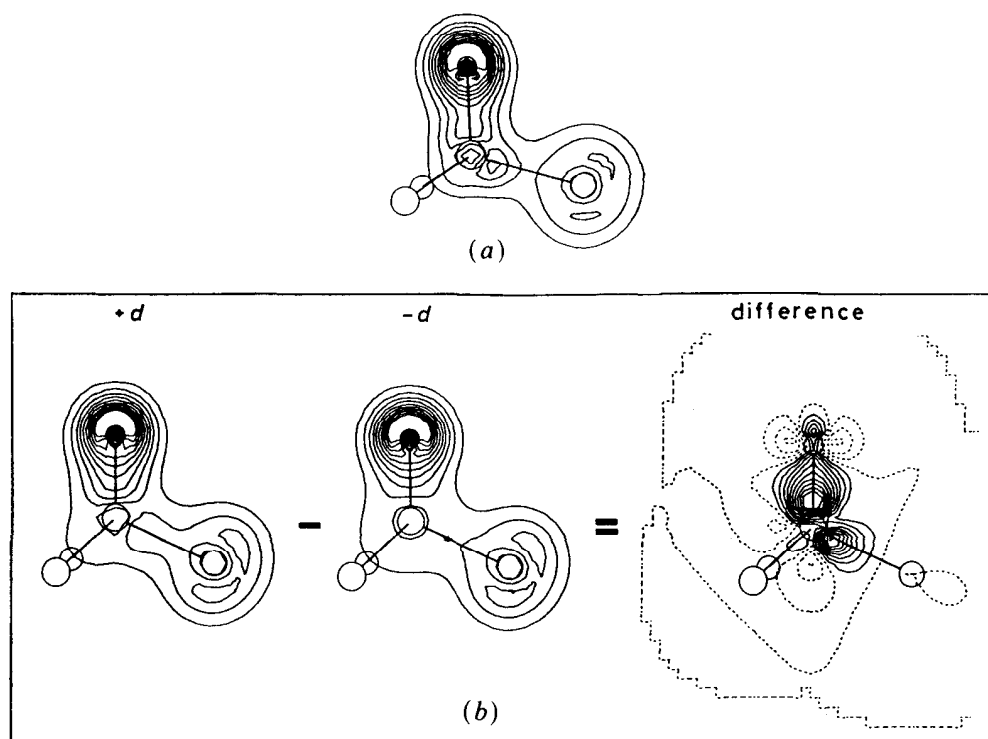


Fig. 4. Total valence-electron-density contour plots for (a) $V(O)Cl_3$ and (b) $P(O)Cl_3$ [calculated with (+ d) and without ($-d$) d atomic orbitals on P]; for the latter the electron-density difference is also plotted to identify d -orbital contributions to the bonding.

Table 2. Effective atomic and overlap charges as well as dipole moments from SCC- $X\alpha$ calculations for PCl_3 , $AsCl_3$ and $E(O)Cl_3$ ($E = P$ or As ; V or Nb). Bond distances d refer to the literature⁹⁻¹² or are estimated

	Q_{eff}			overlap charge		geometry/ \AA			μ_{calc}/D
	E	Cl	O	E—Cl	E—O	$d(E—Cl)$	$d(Cl—Cl)$	$d(E—O)$	
PCl_3^a	0.52	-0.17	—	0.59	—	2.04	3.13	—	0.96
$P(O)Cl_3^b$	0.96	-0.12	-0.59	0.65	1.28	1.99	3.13	1.46	2.61
$AsCl_3^a$	0.80	-0.27	—	0.54	—	2.17	3.28	—	1.78
$As(O)Cl_3^b$	1.20	-0.19	-0.64	0.66	1.34	2.11	3.28	1.57	2.73
$V(O)Cl_3$	1.29	-0.27	-0.48	0.56	1.00	2.14	3.54	1.57	2.22
$Nb(O)Cl_3$	1.14	-0.23	-0.47	0.88	1.37	2.28	3.76	1.68	3.93

^a Without d orbitals in the basis set; ^b including d orbitals in the basis set.

well as calculated dipole moments and the assumed bond distances⁹⁻¹² are listed. Bond polarities are generally more pronounced for $V(O)Cl_3$ and $Nb(O)Cl_3$ compared with the main-group representatives. They decrease on going from vanadium to niobium and increase from phosphorus to related arsenic compounds. This is consistent with increasing covalency from V to Nb and from As to P , *i.e.* for the main-group analogues this effect is reversed.¹⁶ Since overlap charges in table 2 do not differentiate between covalent and ionic contributions to bonds^{5b} this effect is only partly reflected for $V^V \rightarrow Nb^V$; they remain nearly constant for $P^{III} \rightarrow As^{III}$ and $P^V \rightarrow As^V$. The increased covalency from $V(O)Cl_3$ to $Nb(O)Cl_3$ is caused by the

$\pi(p-d)$ -bond overlap charge, which is *ca.* 60% larger for niobium oxytrichloride while the σ -bond charge remains almost constant.

Bonding differences in analogous pairs of main-group and transition-metal compounds will be the subject of future photoelectron-spectroscopic investigations.

We thank the Deutsche Forschungsgemeinschaft for support of this work, Heike Brandstädter for technical assistance and the p.e.s. measurements, and Jens Kudnig for computer software.

- ¹ (a) S. Elbel, J. Kudnig, G. Runger and M. Grodzicki, *J. Electron Spectrosc. Relat. Phenom.*, in press; (b) H. Walther, *D. Phil. Thesis* (Universitat Hamburg, 1983).
- ² S. Elbel and H. tom Dieck, *Z. Anorg. Allg. Chem.*, 1981, **483**, 33.
- ³ (a) S. G. Gibbins, M. F. Lappert, J. B. Pedley and G. J. Sharp, *J. Chem. Soc., Dalton Trans.*, 1975, 72; (b) M. F. Lappert, J. B. Pedley and G. J. Sharp, *J. Organomet. Chem.*, 1974, **66**, 271.
- ⁴ M. Grodzicki, *J. Phys. B*, 1980, **13**, 2683.
- ⁵ (a) R. Blas, M. Grodzicki, V. R. Marathe and A. Trautwein, *J. Phys. B*, 1980, **13**, 2693; (b) M. Grodzicki, H. Walther and S. Elbel, *Z. Naturforsch., Teil B*, 1984, **39**, 1319.
- ⁶ K. Seppelt, D. Lentz and H. H. Eysel, *Z. Anorg. Allg. Chem.*, 1978, **439**, 5.
- ⁷ (a) P. Burroughs, S. Evans, A. Hamnett, A. F. Orchard and N. V. Richardson, *J. Chem. Soc., Faraday Trans. 2*, 1975, **70**, 1899; (b) E. Pellach, G. M. Bancroft and J. S. Tse, *Inorg. Chim. Acta*, 1984, **83**, 93; (c) H. Sambe and R. H. Felton, *Chem. Phys.*, 1981, **59**, 329.
- ⁸ (a) P. J. Bassett and D. R. Lloyd, *J. Chem. Soc., Dalton Trans.*, 1972, 248; (b) P. A. Cox, S. Evans, A. F. Orchard, N. V. Richardson and P. J. Roberts, *Discuss. Faraday Soc.*, 1972, **54**, 26; (c) T. H. Gan, J. B. Peel and G. D. Willett, *Chem. Phys. Lett.*, 1977, **48**, 483; (d) J. C. Bunzli, D. C. Frost and C. A. McDowell, *J. Electron Spectrosc. Relat. Phenom.*, 1973, **1**, 481; (e) I. H. Hillier and V. R. Saunders, *J. Chem. Soc., Dalton Trans.*, 1972, 21; *Chem. Commun.*, 1970, 1510; (f) M. F. Guest, I. H. Hillier and V. R. Saunders, *J. Chem. Soc., Faraday Trans. 2*, 1972, **68**, 867.
- ⁹ K-I. Karakida and K. Kuchitsu, *Inorg. Chim. Acta*, 1975, **13**, 113.
- ¹⁰ L. O. Brockway and F. T. Wall, *J. Am. Chem. Soc.*, 1934, **56**, 2373.
- ¹¹ T. Moritani, K. Kuchitsu and Y. Morino, *Inorg. Chem.*, 1971, **10**, 344.
- ¹² (a) G. Munninghoff, E. Hellner, M. El Essawi and K. Dehnicke, *Z. Kristallogr.*, 1978, **147**, 231; (b) W. Hiller, J. Strahle, H. Prinz and K. Dehnicke, *Z. Naturforsch., Teil B*, 1984, **39**, 107.
- ¹³ W. L. Jorgensen, *Quantum Chemistry Program Exchange*, 1977, **12**, 340.
- ¹⁴ (a) Ying-Nan Chiu and F. E. Wang, *Inorg. Chem.*, 1982, **21**, 4264; (b) J. K. Burdett and T. Hughbanks, *J. Am. Chem. Soc.*, 1984, **106**, 3101.
- ¹⁵ (a) J. Evans, *J. Chem. Soc., Dalton Trans.*, 1980, 1005; (b) S. D. Wijeyesekera and R. Hoffmann, *Inorg. Chem.*, 1983, **22**, 3287; (c) R. H. Summerville and R. Hoffmann, *J. Am. Chem. Soc.*, 1976, **98**, 7240.
- ¹⁶ M. C. Bohm and R. Gleiter, *Angew. Chem.*, 1983, **95**, 334; R. Gleiter, personal communication.
- ¹⁷ S. Elbel and H. tom Dieck, *J. Chem. Soc., Dalton Trans.*, 1976, 1757.
- ¹⁸ (a) J. H. Yates and R. M. Pitzer, *J. Chem. Phys.*, 1979, **70**, 4049; (b) C. E. Myers, L. J. Norman II and L. M. Loew, *Inorg. Chem.*, 1978, **17**, 1581.
- ¹⁹ L. J. Bartolotti, S. R. Gadre and R. G. Parr, *J. Am. Chem. Soc.*, 1980, **102**, 2945.
- ²⁰ L. F. Mattheiss, *Phys. Rev.*, 1964, **134**, A970.
- ²¹ D. J. Kraan, *Phys. Status Solidi B*, 1973, **60**, 587.

(PAPER 4/1353)